Journal of Catalysis **208,** 54–63 (2002)
doi:10.1006/jcat.2002.3523, available online at http://www.idealibrary.com on IDEAL®

Structural Change of Ni Species in Ni/SiO_2 Catalyst during Decomposition of Methane

Sakae Takenaka,[1] Hitoshi Ogihara, and Kiyoshi Otsuka

Department of Applied Chemistry, Graduate School of Science and Engineering, Tokyo Institute of Technology, Ookayama, Meguro-ku, Tokyo 152-8552, Japan

Received July 26, 2001; revised January 15, 2002; accepted January 15, 2002

The structural change of Ni species in a Ni/SiO_2 catalyst during methane decomposition into hydrogen and carbon was investigated by X-ray diffraction (XRD), scanning electron microscopy, and Ni K-edge X-ray absorption near-edge spectroscopy/extended X-ray absorption fine structure (XANES/EXAFS). The Ni/SiO_2 catalyst decomposed methane actively into hydrogen and filamentous carbon at initial periods of the reaction. The catalytic activity for the reaction decreased with time on stream of methane and finally the catalyst was deactivated completely. Prior to the contact of methane with the Ni/SiO_2 catalyst, Ni species on the catalyst were present as Ni metal mainly. XRD analyses showed that Ni metal particles were aggregated as soon as the Ni/SiO_2 came into contact with methane. After this initial aggregation, the structure of the Ni metal did not change appreciably when the Ni/SiO_2 was decomposing methane actively. Ni K-edge XANES/EXAFS suggested the formation of some nickel carbide species on the catalyst when significant deactivation of the catalyst was observed.

Key Words: **silica-supported Ni catalyst; methane decomposition; hydrogen; carbon filament; nickel metal; nickel carbide.**

INTRODUCTION

Hydrogen is a clean fuel in the sense that no CO_2 is emitted when it is used in a H_2–O_2 fuel cell. H_2–O_2 cells such as phosphoric acid and SPE fuel cells require the thorough elimination of carbon monoxide (CO) from the fuel (H_2), because CO poisons strongly the electrocatalysts in the cells. At present, hydrogen is produced mainly through steam reforming and partial oxidation of natural gas. Because the hydrogen produced by these processes inevitably contains CO beyond a tolerable range, removal of CO through a water–gas shift reaction of CO followed by selective CO oxidation should be required. Thus, the purification processes would make the fuel reformer more bulky and expensive.

Decomposition of methane into hydrogen and carbon is of current interest from the viewpoint of an alternative route of hydrogen production from natural gas (1–3). Because no CO was contained in the products obtained by methane decomposition, hydrogen can be utilized directly as the fuel for the H_2–O_2 cells. The carbon formed by the methane decomposition should be used for the synthesis of useful chemicals through gasification with water (4) or CO_2 (5). The carbons can be used also as functional materials, such as fibers, graphite, carbon black, composites, electrodes, and so forth. Recent studies have demonstrated clean hydrogen production via stepwise steam reforming of methane, i.e., decomposition of methane over supported Ni catalyst followed by steam gasification of surface carbon on the catalyst (6, 7).

Concerning catalysts for the decomposition of methane, it is well-known that supported Ni is one of the effective catalysts (8–11). We also confirmed the high catalytic activity and long life of a Ni/SiO_2 catalyst for the decomposition of methane, especially when a fumed silica (Cab–O–Sil) was utilized as a support (12). In general, hydrogen only is formed as a gaseous product and carbons deposited on the catalyst grow with a filamentous structure in the decomposition of methane over a Ni/SiO_2 catalyst. The catalytic activity of Ni/SiO_2 for methane decomposition decreased gradually with time on stream of methane and finally the catalyst was deactivated completely. The reaction mechanisms for methane decomposition over supported Ni catalysts were studied by many research groups (13–16). In these studies, the growth mechanisms of the carbon filaments during methane decomposition were investigated in detail, but little attention was focused on the structural change of Ni species in the catalysts during methane decomposition. We expected that the deactivation of the supported Ni catalyst might be caused by the structural change of Ni species during methane decomposition.

In the present study, we investigated the structural change of Ni species during methane decomposition over Ni/SiO_2 catalysts by means of X-ray diffraction (XRD) and Ni K-edge X-ray absorption near-edge spectroscopy/extended X-ray absorption fine structure (XANES/EXAFS). In addition, the appearance of a Ni/SiO_2 catalyst during methane decomposition was observed by SEM and BEI (back-scattering electron image). Especially, we

[1] To whom correspondence should be addressed. Fax: 81-35734-2879. E-mail: stakenak@o.cc.titech.ac.jp.

0021-9517/02 $35.00

focused on the structural change of Ni species during the deactivation stage of the catalyst and discussed the deactivation mechanism of the catalyst.

EXPERIMENTAL

A silica-supported Ni catalyst (Ni/SiO_2) was prepared by impregnating SiO_2 (Cab–O–Sil; fumed silica obtained from CABOT Co.; specific surface area = 200 $m^2 \cdot g^{-1}$) with an aqueous solution of $Ni(NO_3)_2 \cdot 6H_2O$ at 353 K. The impregnated sample was further dried at 393 K for 12 h and calcined in air at 873 K for 5 h.

The decomposition of methane over the Ni/SiO_2 catalyst was carried out with a gas-flow system at atmospheric pressure. The catalyst was placed at the bottom of a quartz reactor (internal diameters: 2.7 cm for vertical, 2 cm from the bottom, 1.5 cm for upward, 10 cm). Prior to the reaction, the catalyst was reduced with hydrogen at 823 K for 1 h. Decomposition of methane was performed by contacting methane ($P(CH_4) = 101$ kPa, flow rate = 60 ml $\cdot$ min^{-1}) with the catalyst (0.040 g). Hydrogenation of the carbons deposited on the Ni/SiO_2 was carried out successively with the same apparatus after the Ni/SiO_2 catalyst had been deactivated completely for the methane decomposition. The hydrogenation of the carbons predeposited on the Ni/SiO_2 catalyst was initiated by contact with hydrogen ($P(H_2) = 101$ kPa, 70 ml $\cdot$ min^{-1}) at 843 K. During both the decomposition of methane and the hydrogenation of carbons, some of the gases in a stream out of the catalyst-bed was sampled out to analyze the gaseous products by gas chromatography (GC).

X-ray absorption experiments were carried out on the beamline BL-9A at the Photon Factory in the Institute of Materials Structure Science for High Energy Accelerator Research Organization, Tsukuba, Japan, with a ring energy of 2.5 GeV and a stored current of 250–450 mA (Proposal 2000G074). The X-ray absorption spectra of the catalysts were recorded in a fluorescence mode, and those of the reference samples were recorded in a transmission mode with a Si(111) two-crystal monochromator at room temperature. Normalization of XANES and data reduction on EXAFS were performed as described elsewhere (17).

X-ray diffraction (XRD) patterns of the catalysts were measured by a Rigaku RINT 2500V diffractometer using Cu $K\alpha$ radiation.

SEM image and back-scattering electron image of the catalyst were measured using a Hitachi FE-SEM S-800 (field emission gun scanning electron microscope).

RESULTS AND DISCUSSION

Decomposition of Methane over Ni/SiO_2 Catalyst

Figure 1 shows the kinetic curves of formation rates of H_2 in methane decomposition at 803 K over Ni/SiO_2 catalysts

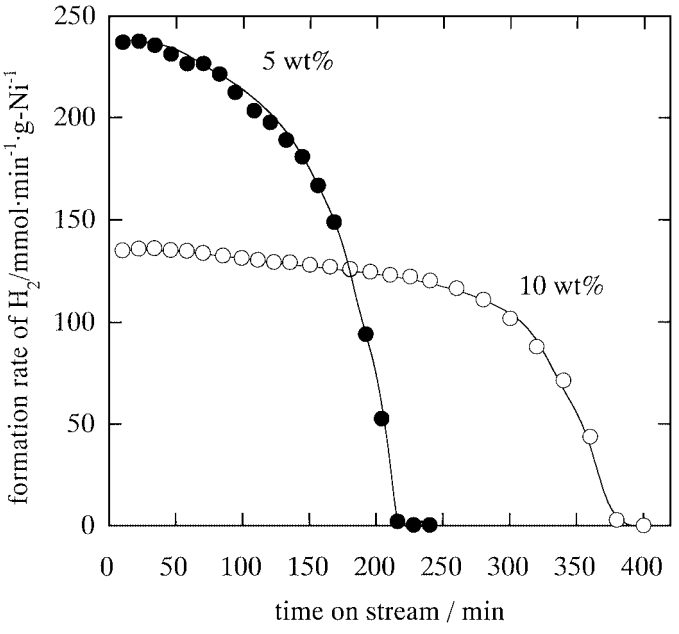

FIG. 1. Kinetic curves of the formation rates of hydrogen in methane decomposition over Ni (5 wt%)/SiO_2 and Ni (10 wt%)/SiO_2 catalysts at 803 K. $P(CH_4)$, 101 kPa; flow rate, 60 ml $\cdot$ min^{-1}; catalyst, 0.040 g.

with loading amount of 5 and 10 wt% as Ni metal. In the reactions, only hydrogen was detected as a gaseous product. In the early period of the reactions, the formation rates of hydrogen were kept high. The rates decreased sharply with time on stream and formation of hydrogen could not be observed at 240 and 400 min of time on stream for Ni (5 wt%)/SiO_2 and Ni (10 wt%)/SiO_2, respectively. The values of C/Ni (the mole of decomposed methane divided by that of all nickel atoms in the catalyst) during complete deactivation of the catalysts were estimated to be 1100 and 1280 for Ni (5 wt%)/SiO_2 and Ni (10 wt%)/SiO_2, respectively.

After the methane decomposition over Ni/SiO_2 catalysts shown in Fig. 1, hydrogenation of the carbons deposited on the catalysts was performed at 843 K. During this hydrogenation, methane only was formed as a gaseous product.

Characterization of the Catalysts by XRD

We measured XRD patterns of the Ni/SiO_2 catalysts after the decomposition of methane in order to investigate the structural changes of Ni species during the reaction. Ni (10 wt%)/SiO_2 was used for the measurements of XRD patterns in order to get diffraction patterns due to Ni species with higher signal-to-noise (S/N) ratios. Prior to measurement of the XRD patterns of the Ni/SiO_2 catalyst, methane decomposition was performed at 803 K over the catalyst. The results are depicted in Fig. 2. In the XRD pattern of the Ni/SiO_2 catalyst after reduction with hydrogen at 823 K (denoted as fresh catalyst), the peaks at 44 and 52° are assigned to Ni metal, indicating that Ni metal particles

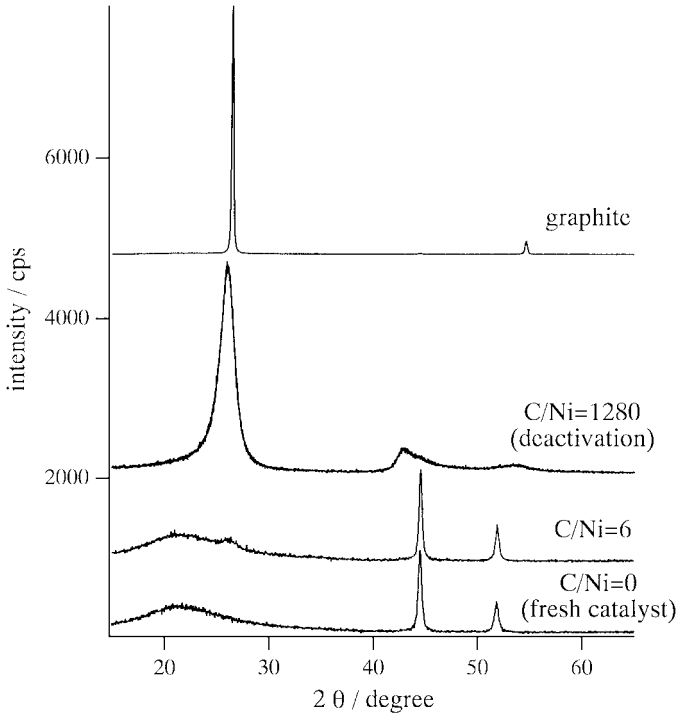

FIG. 2. XRD patterns of graphite and of Ni (10 wt%)/SiO_2 catalysts before and after methane decomposition at 803 K.

are present on the Ni/SiO_2 catalyst before contact with methane. For the XRD pattern of the catalyst with deposited carbons of C/Ni = 6, a small peak was found at 26°. The peak at 26° is assigned to graphite, indicating that the carbon deposited on the Ni/SiO_2 catalyst has a graphitelike structure (4).

Figure 3 shows the change in mean particle size of Ni metal in the Ni (10 wt%)/SiO_2 catalyst at a very early period

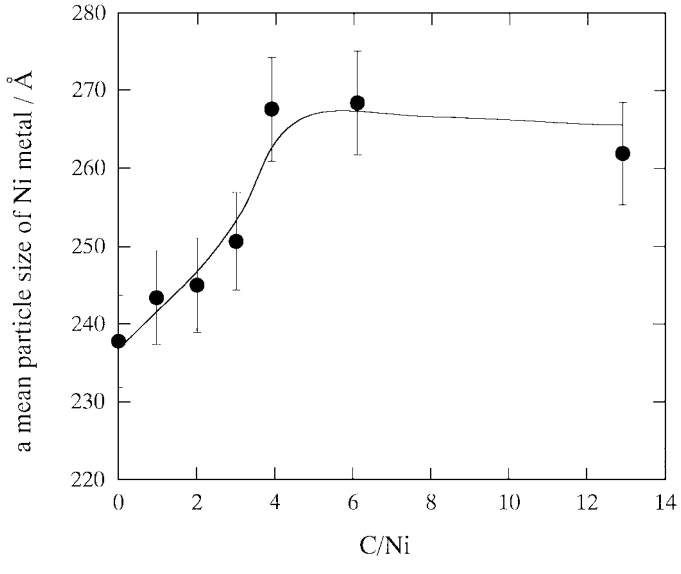

FIG. 3. Change in mean particle size of Ni metal in the Ni (10 wt%)/SiO_2 catalyst during methane decomposition.

of methane decomposition (C/Ni ≤ 14) at 803 K. The mean particle sizes of Ni metal were estimated from full width at half maximum of the diffraction line due to Ni(111) at 44.5° using the Scherrer equation. Before contact of methane with the Ni (10 wt%)/SiO_2 catalyst, the mean particle size of Ni metal was estimated to be 24 nm. On contact of methane with the catalyst, the mean particle sizes of Ni increased from 24 to 27 nm in the range of C/Ni < 4, and the particle size became almost constant in the range of C/Ni > 4. These results suggest that the aggregation of Ni metal particles on the catalyst occurs by contact of methane with the Ni/SiO_2 catalyst.

Figure 2 shows also the XRD pattern of the Ni (10 wt%)/SiO_2 catalyst after complete deactivation for the methane decomposition. In the XRD pattern, the peaks due to graphite structure were observed. It should be noted that the peaks are very broad. Therefore, the crystallinity of the carbon deposited on the catalyst should be low (18). In the XRD pattern of the deactivated Ni/SiO_2 catalyst, no diffraction peak due to Ni species such as Ni metal or some nickel carbide species was observed. This could be due to the formation of amorphous nickel species after complete deactivation of the catalyst or to the low concentration of Ni species in the Ni/SiO_2 catalyst deactivated completely. That is, in the case of methane decomposition over the Ni (10 wt%)/SiO_2 catalyst, the amount of Ni in the catalyst was changed from 10 wt% for the fresh catalyst to 0.4 wt% for the deactivated one due to a large number of deposited carbons.

Ni K-Edge XANES/EXAFS of Ni/SiO_2 Catalyst

Figure 4 shows Ni K-edge XANES spectra of the fresh Ni/SiO_2 catalyst, the catalysts after methane decomposition at 803 K, and a Ni foil. For measurements with Ni K-edge XANES/EXAFS, Ni (5 wt%)/SiO_2 was used. The XANES spectrum of the fresh Ni/SiO_2 (C/Ni = 0) was compatible with that of a Ni foil, indicating that Ni species in the fresh catalyst were present as Ni metal mainly (19). The result was consistent with that deduced from the XRD pattern shown in Fig. 2. The XANES spectra of Ni/SiO_2 catalysts after methane decomposition did not change in the range of C/Ni = 49–650 and the spectra were similar to that of the fresh catalyst. In the range of C/Ni ≤ 650 for methane decomposition over the Ni (5 wt%)/SiO_2 catalyst, the activity of the catalyst was kept high. Therefore, we consider that the structure of Ni species did not change appreciably when the Ni/SiO_2 catalyst was decomposing methane actively.

On the other hand, in the XANES spectrum of the Ni/SiO_2 catalyst with deposited carbons of C/Ni = 900, two shoulder peaks appeared, at 8332 and 8341 eV, and the two peaks became more intense with an increase in C/Ni. Furthermore, two peaks, at 8349 and 8358 eV, which were observed in the XANES spectra of the fresh Ni/SiO_2 catalyst and a Ni foil, became fainter with an increase in C/Ni,

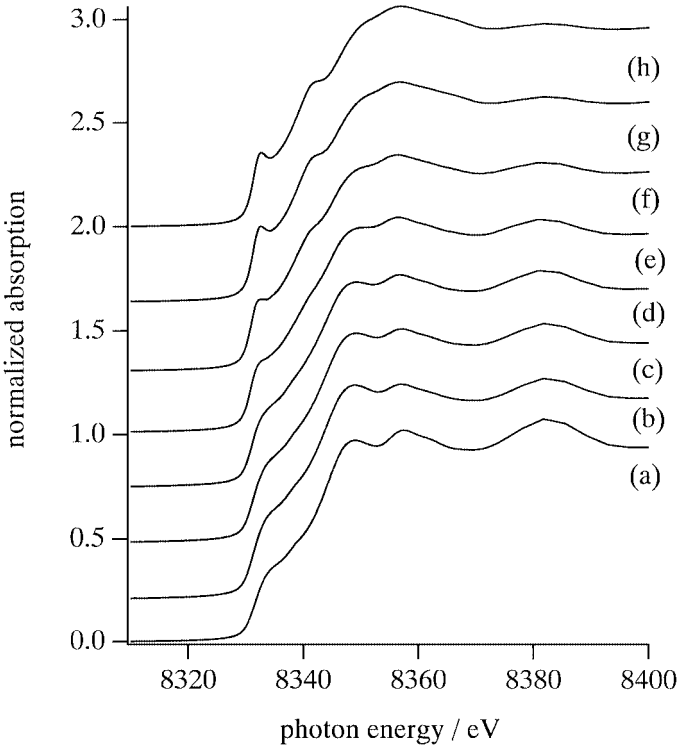

FIG. 4. Ni K-edge XANES spectra of the fresh Ni (5 wt%)/SiO_2 catalyst, the catalysts with carbons deposited by methane decomposition, and a Ni foil. (a) Ni foil, (b) Ni/SiO_2 of C/Ni = 0 (fresh catalyst), (c) C/Ni = 49, (d) C/Ni = 300, (e) C/Ni = 650, (f) C/Ni = 900, (g) C/Ni = 1000, and (h) C/Ni = 1100 (complete deactivation).

in the range C/Ni $\geq$ 900. These results strongly suggest that the structure of Ni species changed significantly in the range C/Ni $\geq$ 900, where the conversion of methane decreased rapidly in methane decomposition over the Ni (5 wt%)/SiO_2 catalyst. Thus, the structural change of Ni species implied by the XANES spectra might be related to the deactivation of the catalyst for methane decomposition.

This structural change of Ni species during the deactivation of the Ni/SiO_2 catalyst could be caused by the formation of nickel carbide species such as Ni_3C (20). In order to examine this hypothesis, a nickel carbide species was prepared by a method in which Ni metal powder comes into contact with CO at 540 K (21). The samples were measured by XRD and Ni K-edge XANES/EXAFS. Figure 5 shows the XRD patterns of the Ni metal powder samples treated with CO at 540 K for 50 and 100 h, and a Ni metal powder. For the XRD patterns of the Ni samples treated with CO, diffraction peaks due to Ni_3C were found at 2θ = 40, 42, 45, 58, 72, and 78°, in addition to peaks due to the Ni metal. The peaks due to Ni_3C became intense with the treatment time with CO. Figure 6 shows the Ni K-edge XANES spectra of the Ni metal powder samples treated with CO, the Ni/SiO_2 catalyst deactivated completely for the methane decomposition, and a Ni foil. On treatment of Ni metal powder with CO, absorption at 8332 eV in the XANES spectra became intense compared with that of Ni foil, and two peaks, at 8349 and 8358 eV, became fainter than those of Ni foil. As described in Fig. 5, Ni_3C was present in the Ni metal powder treated with CO. The formation of Ni–C bonds by treating of Ni metal powder with CO would bring about these changes in the XANES spectra. These changes in the XANES spectra by treating of Ni metal powder with CO were similar to those in the XANES spectra observed during deactivation of the Ni/SiO_2 catalyst (C/Ni $\geq$ 900), as shown in Fig. 4, suggesting the formation of Ni–C bonds in Ni metal particles during deactivation of the Ni/SiO_2 catalyst for methane decomposition.

We further investigated the structural change of Ni species during the deactivation of the Ni/SiO_2 catalyst for methane decomposition by means of XANES spectra of the Ni/SiO_2 catalysts treated with hydrogen. After the Ni (5 wt%)/SiO_2 catalysts had been deactivated completely for methane decomposition at 803 K, the deactivated catalysts were treated with hydrogen at 843 K, which produced methane only. The XANES spectra of the Ni/SiO_2 catalysts thus treated are shown in Fig. 7. Treatment of the deactivated Ni/SiO_2 catalysts with hydrogen brought about the change in the Ni K-edge XANES spectra. The feature of the XANES spectra of the Ni/SiO_2 treated with hydrogen approached gradually that of the fresh catalyst shown in Fig. 4, as carbons deposited on the Ni/SiO_2 catalyst were

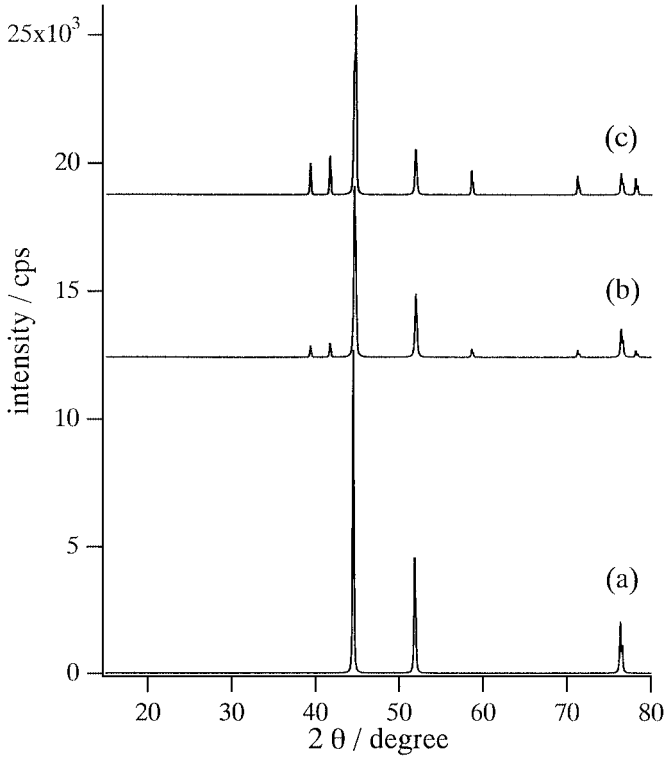

FIG. 5. XRD patterns of Ni metal powder and Ni metal powder samples treated with CO at 540 K. (a) Ni metal powder; (b, c) Ni metal powders treated with CO at 540 K for 50 and 100 h, respectively.

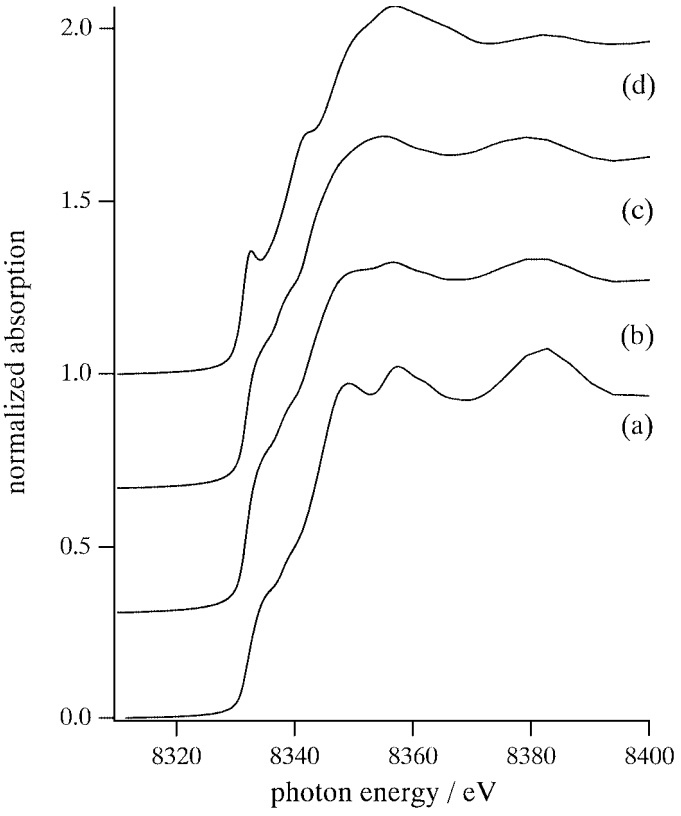

FIG. 6. Ni K-edge XANES spectra of Ni foil (a), Ni metal powder treated with CO at 540 K for 50 (b) and 100 h (c), and the Ni (5 wt%)/SiO_2 catalyst deactivated completely by the methane decomposition at 803 K (d).

hydrogenated into methane. The intensities of shoulder peaks at 8332 and 8341 eV, which had appeared during the serious deactivation of the catalyst (C/Ni $\geq$ 900) for the methane decomposition (Fig. 4), became weak, and two peaks, at 8349 and 8358 eV, which were observed in the XANES spectra of the fresh Ni/SiO_2 and Ni foil, became clearer on the hydrogenation of carbons. These results indicate that Ni species on the deactivated Ni/SiO_2 catalyst are recovered to Ni metal by treatment with hydrogen. The treatment of the deactivated catalyst with hydrogen produced methane only and brought about the changing of some Ni species in the deactivated catalyst to Ni metal. Therefore, we consider that the structural change of Ni species in the Ni/SiO_2 catalyst during the serious deactivation for methane decomposition was caused by the carbon atoms deposited, i.e., the formation of some nickel carbide species.

Figure 8 shows k^3-weighted Ni K-edge EXAFS spectra of the Ni (5 wt%)/SiO_2 catalysts before and after methane decomposition at 803 K. The feature of the EXAFS spectra of the fresh Ni/SiO_2 catalyst was compatible with that of Ni foil, indicating that Ni species on the fresh Ni/SiO_2 was present as Ni metal mainly (19), as described in Fig. 4. For EXAFS spectra of the Ni/SiO_2 catalyst with deposited carbons of C/Ni = 49–650, the intensity and pattern of the oscillation were almost consistent with those of the EXAFS spectra of the fresh Ni/SiO_2 catalyst. Therefore, the structure of Ni metal on the Ni (5 wt%)/SiO_2 did not change appreciably in the range of C/Ni = 49–650 of the methane decomposition. On the other hand, in the range of C/Ni $\geq$ 900, the intensities of the oscillation of the EXAFS spectrum became smaller with an increase in C/Ni, although the pattern of the oscillation did not change with the values of C/Ni. These results may imply a slight distortion of the structure of Ni metal during the significant deactivation of the Ni (5 wt%)/SiO_2 for the decomposition of methane (C/Ni $\geq$ 900).

Figure 9 shows k^3-weighted Ni K-edge EXAFS spectra of the Ni (5 wt%)/SiO_2 with deposited carbons. The Ni/SiO_2 catalysts, which had been deactivated for the methane decomposition, were treated with hydrogen at 843 K. The amplitude of the EXAFS oscillation of the deactivated Ni/SiO_2 catalyst became more intense as the hydrogenation of carbons deposited on the catalyst into methane proceeded. The result suggests that the distortion of the structure of Ni species observed in the deactivated Ni/SiO_2 catalyst was removed by the treatment with hydrogen. This indicates that

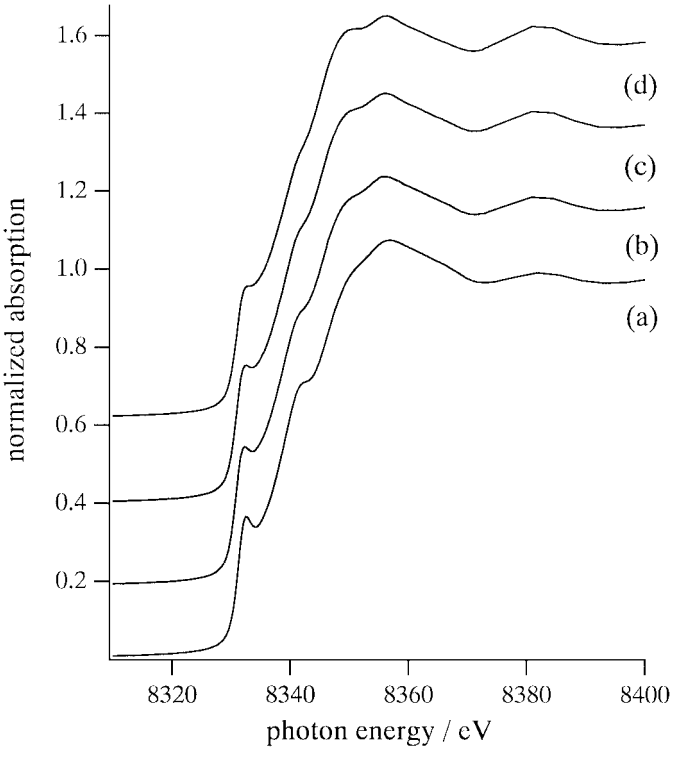

FIG. 7. Ni K-edge XANES spectra of Ni (5 wt%)/SiO_2 catalysts with deposited carbons. (a) The Ni/SiO_2 catalyst after complete deactivation for the methane decomposition at 803 K (C/Ni = 1100). (b–d) Carbons on Ni/SiO_2 catalysts which had been deactivated completely for methane decomposition (C/Ni = 1100) were hydrogenated into methane at 843 K to C/Ni = 1090, 1070, and 1020, respectively.

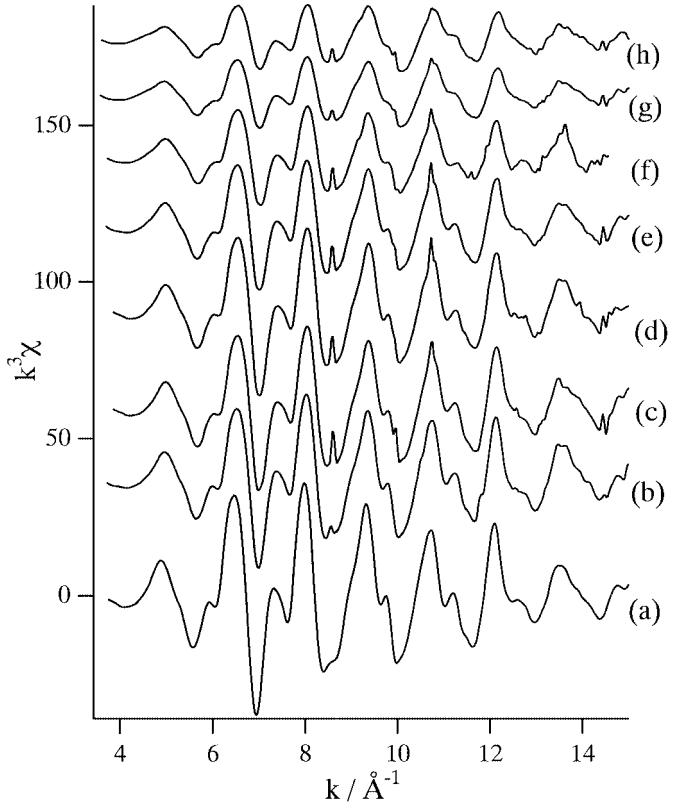

FIG. 8. k^3-weighted Ni K-edge EXAFS spectra of Ni (5 wt%)/SiO_2 catalysts with deposited carbons. (a) Ni foil, (b) C/Ni = 0 (the fresh catalyst), (c) C/Ni = 49, (d) C/Ni = 300, (e) C/Ni = 650, (f) C/Ni = 900, (g) C/Ni = 1000, and (h) C/Ni = 1100 (deactivated catalyst).

the carbon atoms deposited on the catalyst cause the distortion of the structure of Ni metal. This could be ascribed to the formation of some nickel carbide species during the significant deactivation of the Ni/SiO_2 catalyst for the methane decomposition, as suggested earlier.

The EXAFS spectra of the Ni metal powder samples treated with CO for 50 and 100 h are shown in Figs. 9e and 9f, respectively. In the EXAFS spectra of the Ni metal powder samples treated with CO, the intensities of the oscillations at 6.0, 7.5, 9.8, and 11.2 Å^{-1} are stronger than those of the EXAFS spectra of the deactivated Ni/SiO_2 catalyst. In addition, the intensities at 6.0, 7.5, 9.8, and 11.2 Å^{-1} became stronger as the time for the treatment of Ni metal powder with CO was lengthened. The feature of these EXAFS spectra of Ni samples treated with CO, which consist of a mixture of Ni metal and Ni_3C, was quite different from that of the EXAFS spectra of the deactivated Ni/SiO_2 catalyst. Therefore, the nickel carbide species present on the deactivated Ni/SiO_2 catalyst was not a Ni_3C compound itself.

Data on the structural changes around Ni atoms during methane decomposition have been strongly supported by performing Fourier transform for k^3-weighted EXAFS of the Ni/SiO_2 catalysts, shown in Figs. 8 and 9. Figure 10 shows the Fourier transforms (radial structure function (RSF)) of k^3-weighted Ni K-edge EXAFS of Ni (5 wt%)/SiO_2 catalysts without and with deposited carbons, and Ni foil. A peak due to Ni–Ni bond was observed at 1.8–2.5 Å in all RSFs in Fig. 10. In the range of C/Ni $\geq$ 900, the intensities of the peak due to Ni–Ni became smaller gradually with an increase in C/Ni, whereas the significant change in the intensity of the peak was not observed in the range of C/Ni $\leq$ 650. In addition, a peak was found at 1.2–1.8 Å in the RSFs of the Ni/SiO_2 catalysts with deposited carbons of more than C/Ni = 900, and the peak became more intense with an increase in the C/Ni. This peak should be ascribed to a Ni–C bond, taking into account the results of the XANES described above.

Figure 11 depicts the Fourier transforms of the Ni/SiO_2 catalyst treated with hydrogen after complete deactivation for the methane decomposition. It was found that the intensities in the peak due to a Ni–Ni bond at 1.9–2.7 Å became stronger as the carbons deposited on the catalyst were

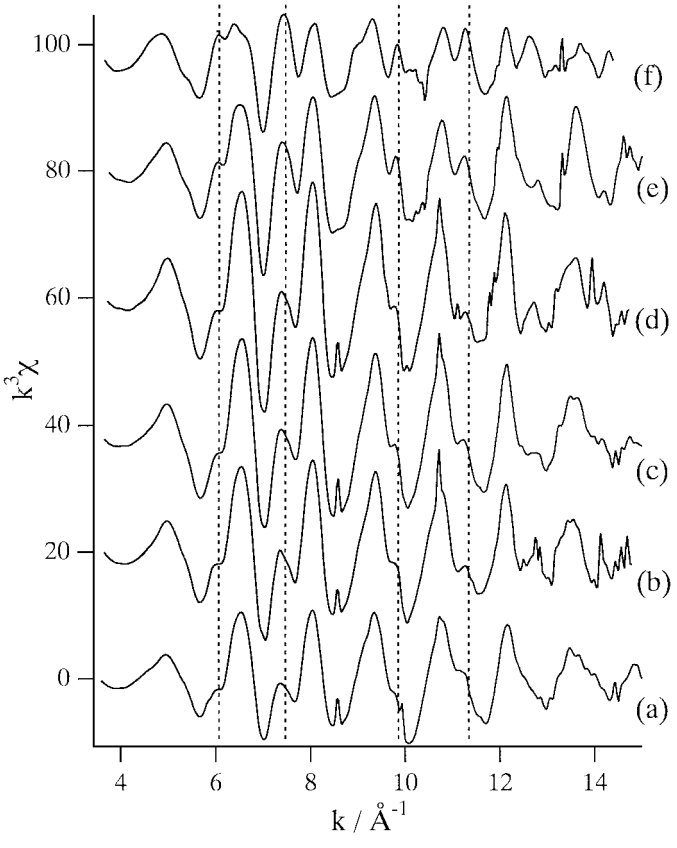

FIG. 9. k^3-weighted Ni K-edge EXAFS spectra of Ni (5 wt%)/SiO_2 catalysts with deposited carbons, and Ni samples treated with CO at 540 K. (a) The Ni/SiO_2 catalyst after complete deactivation for the methane decomposition (C/Ni = 1100). (b–d) Carbons on Ni/SiO_2 catalysts which had been deactivated for methane decomposition (C/Ni = 1100) were hydrogenated at 843 K to C/Ni = 1090, 1070, and 1020, respectively. (e, f) Ni metal powders treated with CO at 540 K for 50 and 100 h, respectively.

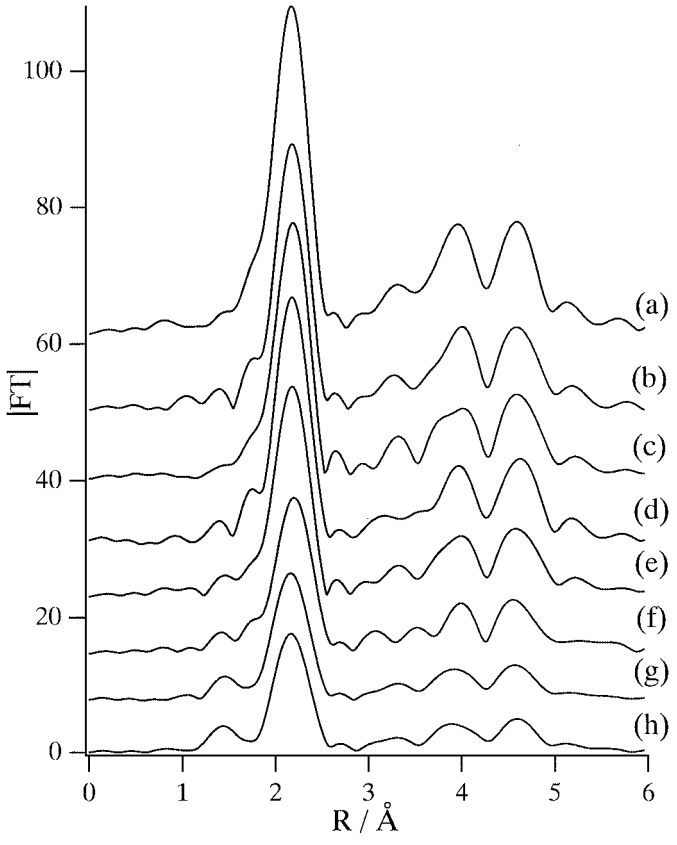

FIG. 10. Fourier transforms of k^3-weighted Ni K-edge EXAFS spectra of Ni (5 wt%)/SiO_2 catalysts with deposited carbons. (a) Ni foil, (b) C/Ni = 0 (the fresh catalyst), (c) C/Ni = 49, (d) C/Ni = 300, (e) C/Ni = 650, (f) C/Ni = 900, (g) C/Ni = 1000, and (h) C/Ni = 1100 (deactivated catalyst).

hydrogenated into methane (Figs. 11a–11d). These results indicate that the treatment of the deactivated catalyst with hydrogen brings about the change of nickel carbide species to Ni metal.

SEM Images of Ni/SiO_2 Catalysts

Figure 12 shows the SEM images and BEIs (backscattering electron images) of the Ni (5 wt%)/SiO_2 with deposited carbons of C/Ni = 1 and 10. The BEIs were measured at the same time as the SEM pictures shown on left side. The BEIs in Fig. 12 show a number of bright spots. The spots indicate the presence of Ni atoms on the catalysts. In the SEM pictures in the range of C/Ni $\leq$ 10, no carbon filament was observed on the catalyst, while in the range of larger values of C/Ni, deposited carbons from the methane decomposition grew with filamentous structure, as is described later.

In the range of C/Ni $\leq$ 10, it was found that a mean particle size of Ni metal became larger with an increase in C/Ni, as shown in Fig. 3. The observation strongly suggests that Ni metals would be aggregated and crystallized firmly by the contact of methane with Ni/SiO_2, forming larger crystal sizes of Ni metal particles than that on the fresh catalyst, before the formation of carbon filaments. The aggregation of Ni species on contact with methane was also observed in the case of a nickel–magnesia catalyst (23) and Ni/Al_2O_3 catalyst (24).

Figure 13 depicts the SEM images and BEIs of the Ni/SiO_2 catalysts with deposited carbons of C/Ni = 49, 200, and 600. In the range of C/Ni = 49–600, the activity of the Ni (5 wt%)/SiO_2 catalyst for the methane decomposition was kept high. In the SEM picture of the Ni/SiO_2 catalyst with deposited carbons of C/Ni = 49, it was found that carbons on the catalyst grew with a filamentous structure (4, 9–16). The filamentous carbons became longer as the value of C/Ni increased. All the BEIs in Fig. 13 show that a Ni metal particle is present on the tip of each carbon filament (4, 9–16). The Ni metal on the tip of the carbon filament decomposes methane and grows the length of the carbon filament successively.

The Ni K-edge XANES spectra of the Ni/SiO_2 with deposited carbons of C/Ni = 49–650 indicated almost the same feature irrespective of the C/Ni value (Fig. 4). In addition,

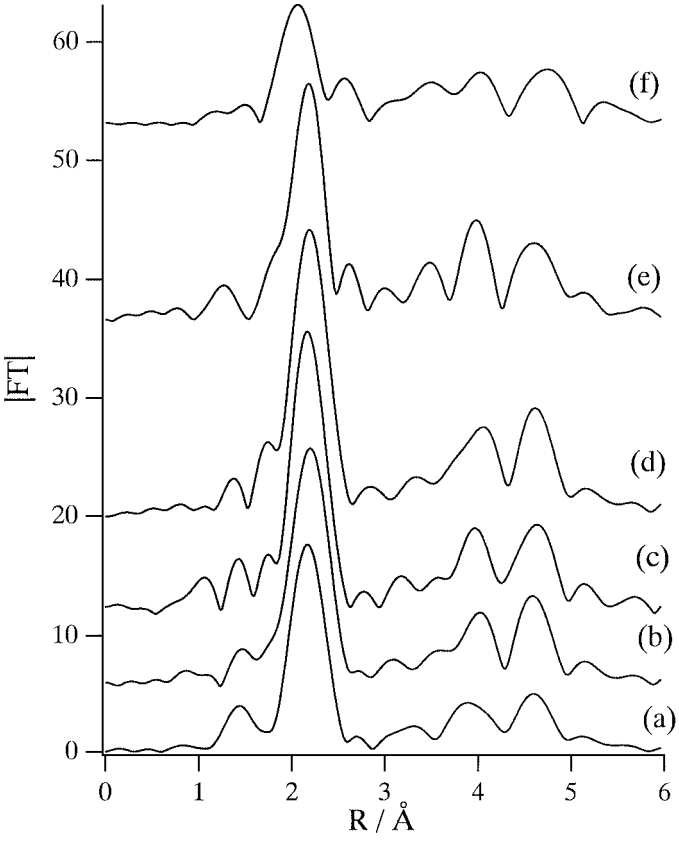

FIG. 11. Fourier transforms of k^3-weighted Ni K-edge EXAFS spectra of Ni (5 wt%)/SiO_2 catalysts with deposited carbons, and Ni samples treated with CO at 540 K. (a) The deactivated catalyst (C/Ni = 1100); (b–d) the Ni/SiO_2 catalysts after the hydrogenation of deposited carbons from C/Ni = 1100 to 1090, 1070, and 1020, respectively; (e, f) Ni samples treated with CO at 540 K for 50 and 100 h, respectively.

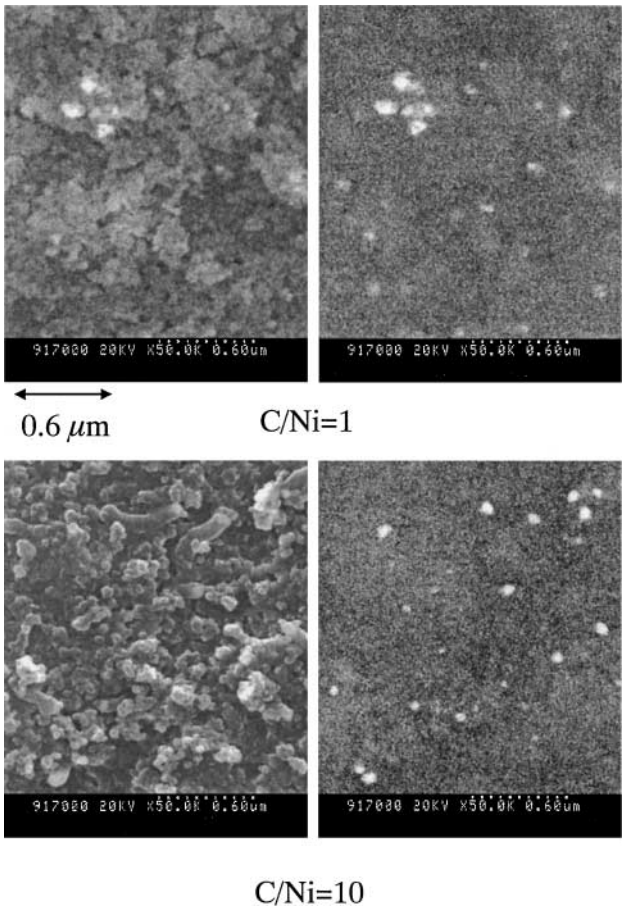

FIG. 12. SEM and BEIs of Ni (5 wt%)/SiO_2 catalysts with carbons deposited of C/Ni = 1 and 10. The carbons were deposited on the Ni (5 wt%)/SiO_2 catalyst by methane decomposition at 803 K.

the pattern and amplitude of the EXAFS oscillation of Ni/SiO_2 with deposited carbons did not change in the range of C/Ni = 49–650 (Fig. 8). These results suggested that the structure of Ni metal did not change when the catalytic activity of Ni/SiO_2 for the methane decomposition was kept high.

Figure 14 shows SEM images and BEIs of the Ni/SiO_2 catalysts with deposited carbons of C/Ni $\geq$ 900. In the range of C/Ni $\geq$ 900, the Ni (5 wt%)/SiO_2 catalyst was deactivated significantly. In the SEM images, collisions between the side wall of a carbon fiber and a Ni particle on the tip of another carbon fiber were found. In SEM images of the Ni/SiO_2 catalysts with deposited carbon of C/Ni $<$ 900, some tips of carbon fibers were found, as shown in Fig. 13, while the number of nickel particles seen was decreased in SEM images of the samples of C/Ni $\geq$ 900. This may be the result of the collision between carbon filaments and the Ni particles at the tips of the filament. However, we cannot exclude the possibility that dilution of the Ni particles due to the growth of carbon fibers also decreases the number of particles in the visual field of the SEM. The images of the deactivated Ni/SiO_2 shown in Fig. 14 indicate that a nickel metal on the tip of a carbon fiber was covered with carbon layers (in the circle in the SEM). The deposited carbon layers on the surface of the Ni metal should interfere with the contact of methane with Ni metal.

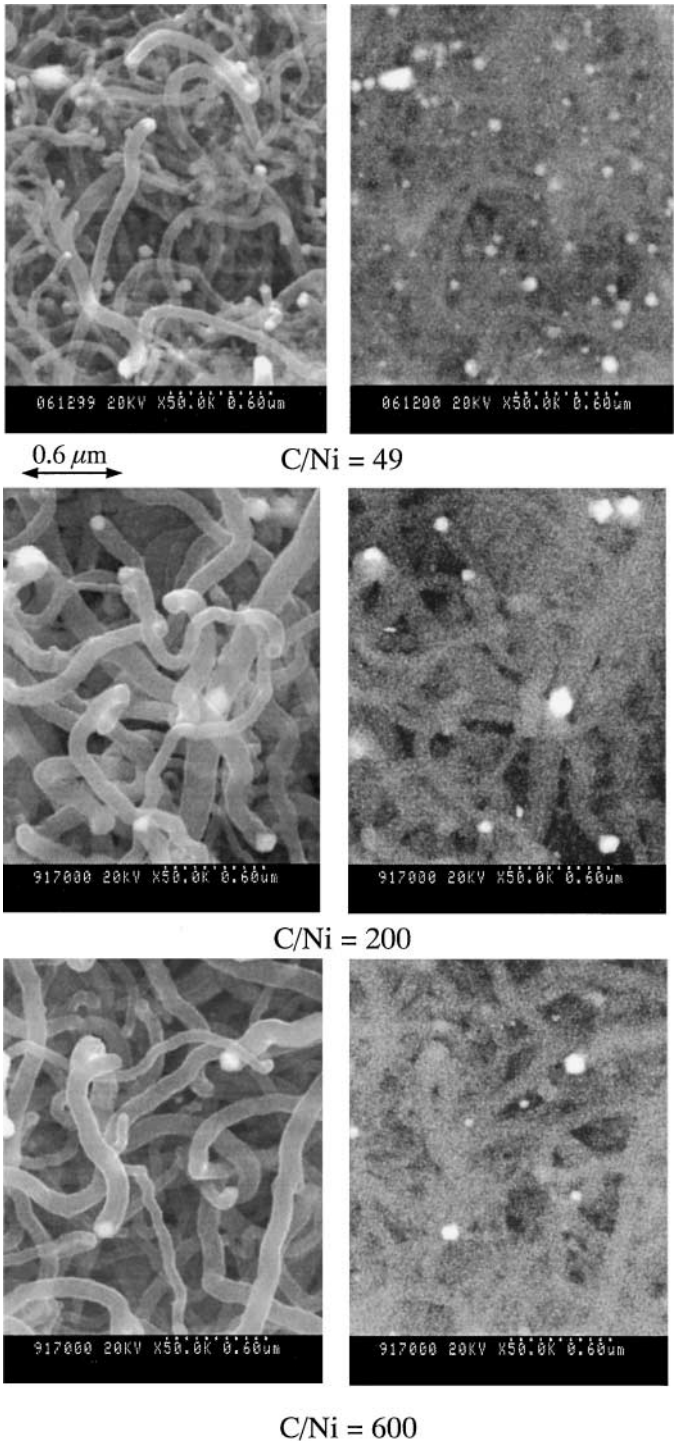

FIG. 13. SEM and BEIs of Ni (5 wt%)/SiO_2 catalysts with deposited carbons of C/Ni = 49, 200, and 600. The carbons were deposited on the Ni (5 wt%)/SiO_2 catalysts by methane decomposition at 803 K.

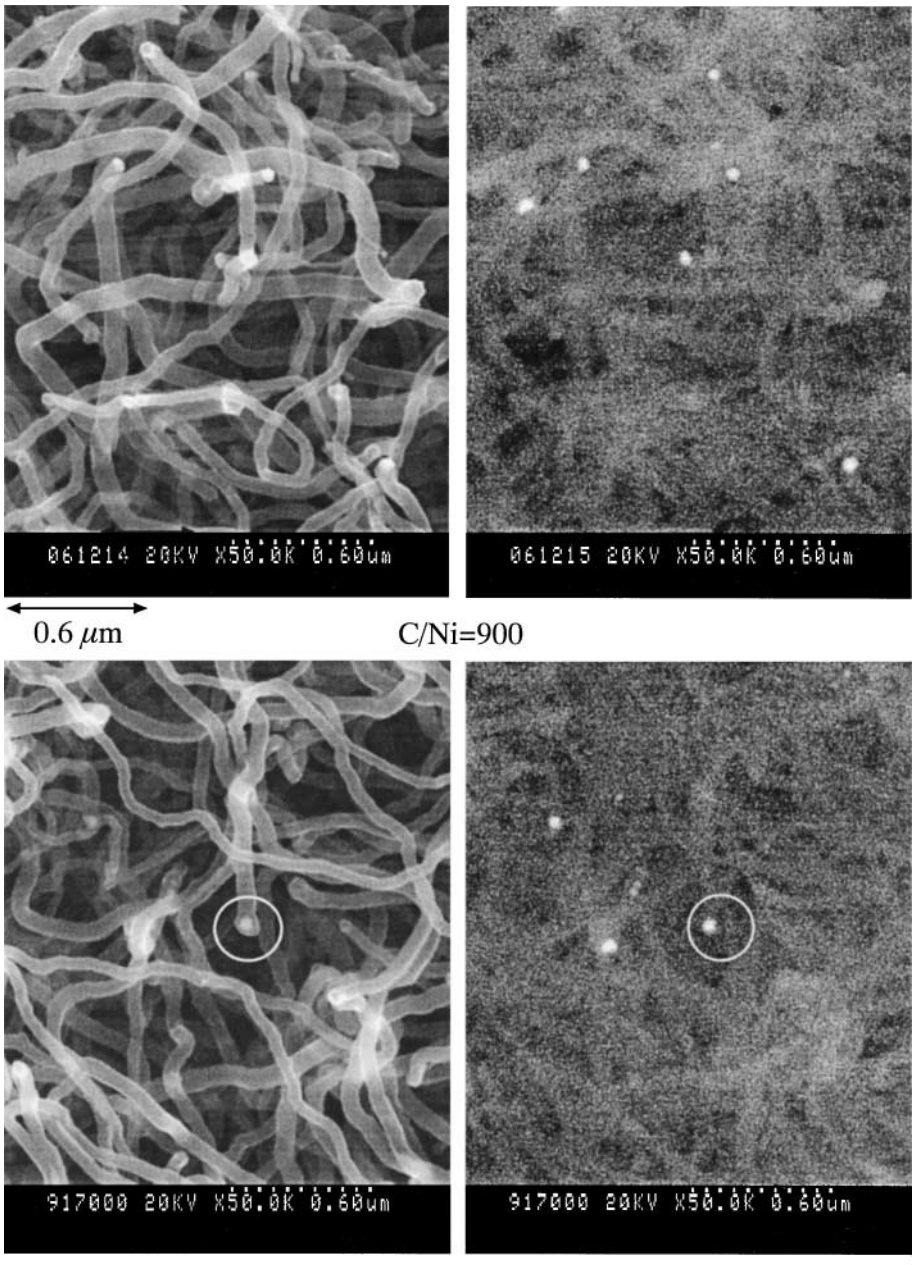

FIG. 14. SEM and BEIs of Ni (5 wt%)/SiO_2 catalysts with deposited carbons of C/Ni = 900 and 1100 (deactivated catalyst). The carbons were deposited on the Ni (5 wt%)/SiO_2 catalysts by methane decomposition at 803 K.

In the XANES spectra of the Ni/SiO_2 catalyst with deposited carbon of C/Ni = 900, two shoulder peaks appeared, at 8332 and 8341 eV, and the two peaks became more intense with an increase in C/Ni, as shown in Fig. 4. The amplitude of EXAFS oscillations of the Ni/SiO_2 catalysts became weaker with an increase in C/Ni, in the range of C/Ni $\geq$ 900. In addition, a peak which would be due to Ni–C appeared at 1.4 Å in the Fourier transforms of the Ni/SiO_2 with deposited carbons of C/Ni $\geq$ 900 (Fig. 10). From the results described above, we concluded that some nickel carbide species were formed on the Ni/SiO_2 catalyst during the significant deactivation period in the methane decomposition. The shoulder peaks at 8332 and 8341 eV which appeared in the XANES spectra of the deactivated Ni/SiO_2 catalysts would be assigned to the transition of an electron from Ni 1s to antibonding Ni–C. The density of carbon atoms in the Ni metal became higher as the catalyst was more and more deactivated. Thus, the intensity of the

two shoulder peaks in the XANES should be stronger with the value of C/Ni. The increase in the density of carbon atoms in the Ni metal during the deactivation of Ni/SiO_2 should cause the distortion of the structure of Ni metal. The decrease in the amplitude of the EXAFS oscillations of the Ni/SiO_2 during the deactivation period can be ascribed to interference between the slightly different environments of the Ni–Ni bonds for Ni metal and nickel carbide species. The formation of a nickel carbide species was also suggested from the experiments with the deactivated Ni/SiO_2 catalyst treated with hydrogen. On treatment with hydrogen, the XANES and EXAFS spectra of the deactivated catalyst were changed to those of the catalysts before deactivation (Figs. 7, 9, and 11). Methane was the only product in this hydrogen treatment for the deactivated catalyst. The reaction between the nickel carbide species with hydrogen must produce methane, regenerating Ni metals.

On the other hand, the XANES and EXAFS spectra of the Ni sample composed of Ni metal and Ni_3C were different from those of the deactivated Ni/SiO_2 catalyst (Figs. 6, 9, and 11). Therefore, the nickel carbide species formed on the Ni/SiO_2 catalyst during the deactivation period of the catalyst for the methane decomposition was different from Ni_3C. In previous reports, it was reported that nickel carbide species were unstable at high temperatures and decomposed into carbon and Ni metal, although the carbide species should be present and/or carbon atoms dissolved in Ni metal during the contact of hydrocarbon with Ni metal at high temperatures (24, 25). On the other hand, Motojima *et al*. reported that Ni_3C was formed when Ni metal came into contact with C_2H_2 at 1023 K (20). In the present study, we cannot explain these discrepancies.

At the moment, we consider that the Ni/SiO_2 catalyst can be deactivated by the collision of an active Ni metal on the tip of a carbon fiber with other carbon fibers, as well as by the coating of a Ni metal surface with deposited carbon layers (26), as found in SEM images (Fig. 14). The collision between the carbon filaments and/or the coating of a Ni metal surface with carbon would cause the formation of a nickel carbide species.

CONCLUSION

We conclude as follows from the results mentioned above.

1. Ni metal particles are aggregated and crystallized firmly by the contact of methane with Ni/SiO_2, forming larger crystal sizes of Ni metal particles than that on the fresh catalyst.

2. The structure of Ni metal does not change significantly when the Ni/SiO_2 catalyst decomposes methane actively.

3. Ni species are changed from Ni metal to some Ni carbide species during the deactivation period of the Ni/SiO_2 catalyst for methane decomposition.

ACKNOWLEDGMENTS

The X-ray absorption experiment was performed under the approval of the Photon Factory Program Advisory Committee (Proposal 2000G074). The authors thank Prof. T. Tanaka in Kyoto University for kind help with the X-ray absorption spectra.

REFERENCES

1. Muradov, N. Z., *Int. J. Hydrogen Energy* **18**, 211 (1993).
2. Gaudernack, B., and Lynum, S., *Int. J. Hydrogen Energy* **23**, 1087 (1998).
3. Choudhary, T. V., Sivadinarayana, C., Chusuei, C. C., Klinghoffer, A., and Goodman, D. W., *J. Catal*. **199**, 9 (2001).
4. Zhang, T., and Amiridis, M. D., *Appl. Catal. A* **167**, 161 (1998).
5. Takenaka, S., and Otsuka, K., *Chem. Lett*. 218 (2001).
6. Choudhary, T. V., and Goodman, D. W., *J. Catal*. **192**, 316 (2000).
7. Aiello, R., Fiscuc, J. E., zur Loye, H.-C., and Amiridis, M. D., *Appl. Catal. A* **192**, 227 (2000).
8. Ishihara, T., Miyashita, Y., Iseda, H., and Takita, Y., *Chem. Lett*. 93 (1995).
9. Ermakova, M. A., Ermakov, D. Yu., Kuvshinov, G. G., and Plyasova, L. M., *J. Catal*. **187**, 77 (1999).
10. Shaikhutdinov, Sh. K., Avdeeva, L. B., Goncharova, O. V., Kochubey, D. I., Novgorodov, B. N., and Plyasova, L. M., *Appl. Catal. A* **126**, 125 (1995).
11. Otsuka, K., Kobayashi, S., and Takenaka, S., *Appl. Catal. A* **190**, 261 (2000).
12. Otsuka, K., Seino, T., Kobayashi, S., and Takenaka, S., *Chem. Lett*. 1179 (1999).
13. Baker, R. T. K., Barber, M. A., Harris, P. S., Feates, F. S., and Waite, R. J., *J. Catal*. **26**, 51 (1972).
14. Tavares, M. T., Alstrup, I., Bernardo, C. A., and Rostrup-Nielsen, J. R., *J. Catal*. **147**, 525 (1994).
15. Ermakova, M. A., Ermakov, D. Yu., and Kuvshinov, G. G., *Appl. Catal. A* **201**, 61 (2000).
16. Ferelonov, V. B., Derevyankin, A. Yu., Okkel, L. G., Avdeeva, L. B., Zaikovskii, V. I., Moroz, E. M., Salanov, A. N., Rudia, N. A., Likholobov, V. A., and Shaikhutdinov, Sh. K., *Carbon* **35**, 1129 (1997).
17. Yoshida, S., Takenaka, S., Tanaka, T., Hirano, H., and Hayashi, H., *Stud. Surf. Sci. Catal.* **101**, 871 (1996).
18. Takenaka, S., Ogihara, H., Yamanaka, I., and Otsuka, K., *Appl. Catal. A* **217**, 101 (2001).
19. Shido, T., Lok, M., and Prins, R., *Top. Catal*. **8**, 223 (1999).
20. Motojima, S., Asakura, S., Hirata, M., and Iwanaga, H., *Mater. Sci. Eng. B* **34**, 9 (1995).
21. Hoffer, L. J. E., Cohn, E. M., and Peebles, W. C., *J. Phys. Colloid Chem*. **54**, 1161 (1950).
22. Espinos, J. P., Gonzalez-Elipe, A. R., Munuera, G., Garcia, J., Conesa, J. C., and Burattini, E., *Physica B* **158**, 174 (1989).
23. Tomishige, K., Chen, Y. G., and Fujimoto, K., *J. Catal*. **181**, 91(1999).
24. Avdeeva, V. B., Goncharova, O. V., Kochubey, D. I., Zaikovskii, V. I., Plyasova, L. M., Novgorodov, B. N., and Shaikhutdinov, Sh. K., *Appl. Catal. A* **141**, 117 (1996).
25. Kock, A. J. H. M., de Bokx, P. K., Boellaard, E., Klop, W., and Geus, J. W., *J. Catal.* **96**, 468 (1985).
26. Kuijpers, E. G. M., Tjepkema, R. B., and Geus, J. W., *J. Mol. Catal*. **25**, 241 (1984).